

Influence of twinning planes on the spectrum of the electron–phonon interaction in tin

A. V. Khotkevich, I. K. Yanson, M. B. Lazareva, V. I. Sokolenko, and Ya. D. Starodubov

Physicotechnical Institute, Academy of Sciences of the Ukrainian SSR, Kharkov

(Submitted 4 February 1990; resubmitted 27 April 1990)

Zh. Eksp. Teor. Fiz. **98**, 1672–1679 (November 1990)

An anomalous softening of the spectrum of the electron–phonon interaction was observed experimentally at point microcontacts between tin single crystals containing twinning planes. Observations revealed a reduction (untypical of samples free of twinning planes) in the average phonon frequency, which was due to an increase in the relative intensity in the I_f part of the spectrum, an increase in the background component of the spectrum, and retention of its high absolute intensity. Estimates of an increase in the superconducting transition temperature δT_c for a metal layer near a twinning plane gave $\delta T_c \sim T_c$.

INTRODUCTION

It was first pointed out in Ref. 1 that the reason for the increase in the superconducting transition temperature T_c is the presence of twin layers formed as a result of low-temperature deformation of a superconductor and that the phonon spectrum as well as the electron–phonon interaction (EPI) constant change the coherent boundaries of such layers at distances of the order of several atomic spacings. It was suggested in Ref. 2 that a “two-dimensional metal” layer exists near a twinning plane and that such a layer has its own characteristic two-dimensional group of electrons and a phonon branch, where the conditions ensuring an increase in T_c may be realized. These reports stimulated intensive experimental and theoretical investigations of the superconductivity of twinning planes and the results of these are summarized in a review paper of Khlyustikov and Buzdin.³

As pointed out recently,⁴ the critical temperature of the onset of the superconductivity of twinning planes can be not only higher, but also lower than the corresponding critical temperature of the bulk superconductivity, depending on the density of natural defects in twinning planes. The mechanism responsible for the change in the critical temperature near twinning planes and the actual form of the energy spectra of quasiparticles (electrons and phonons), as well as the form of the EPI spectrum in a thin metal layer adjoining a twinning plane are not yet known.³ We carried out an experimental study of the EPI near twinning planes by the method of point-contact spectroscopy in the normal state⁵ and thus obtained information on the EPI in the bulk of the metal covering a region with linear dimensions of the order of the point-contact diameter which in turn could be made comparable with the effective thickness of a twinning plane. We assumed that the results obtained could be important in checking the hypotheses used in the interpretation of the experiments on the superconductivity of twinning planes and also for the development of a relevant theory.

GEOMETRY OF SAMPLES AND EXPERIMENTAL PROCEDURE

We investigated the characteristics of pressure point microcontacts of the sliding type (Ref. 5),¹⁾ formed in liquid helium by soft contact of two parallelepiped electrodes along their edges (Fig. 1a) and a subsequent displacement of one electrode relative to the other in the contact plane (Fig.

1b). This method avoided deformation of a metal, known to occur in pressure contacts formed simply by pressing the electrodes together. Here we can easily see from Fig. 1b that when the direction of the mutual displacement of the electrodes in the plane of their contact lay between the directions of the generators of the side surfaces of each of the electrodes, each pair of electrodes could be used to form, in the same cycle, a large number of contacts between new parts of the surface of each of the electrodes along the whole length.

When a system of parallel twinning planes was oriented perpendicularly or at some angle relative to the longitudinal axis of one of the electrodes (Figs. 1a and 1b), the adopted contact-formation method ensured a finite probability of a point of emergence of twinning planes on the surface of a sample within the contact region (Fig. 1c). This probability was governed both by the distance between twinning planes and by the contact diameter, and it could be doubled if identical systems of twinning planes reached both electrodes. Clearly, when the distance between the twinning planes in each of the electrodes was much greater than the contact diameter, the probability that each bank formed by an electrode was simultaneously in contact with twinning planes was considerably less than the probability of formation of a contact containing just one twinning plane (Fig. 1c). In this experimental setup the anomalies of the characteristics of some of the contacts were observed naturally when one of the electrodes was in contact with twinning planes. The expected number of contacts with twinning planes was governed by the total number of consecutively formed contacts and by the probability establishing one contact with a twinning plane.

Electrode blanks were of 1.5×1.5 mm cross-section and they were cut by spark machining from a tin single crystal characterized by $R_{300\text{ K}}/R_{4.2\text{ K}} \approx 4 \cdot 10^4$. Before cutting up into electrodes of 10 mm length some of the blanks were deformed by stretching at 77 K. This deformation created mainly $\{301\}$ twinning planes oriented at approximately 45° to the electrode contact plane (Fig. 1c). The average distance between twinning planes measured with an optical microscope was $5 \times 10^{-3} - 10^{-4}$ cm, which was an order of magnitude greater than the minimum controlled distance along the electrode edges between neighboring contacts, which were formed consecutively using a mechanical micro-positioning device. The electrodes were not heated above

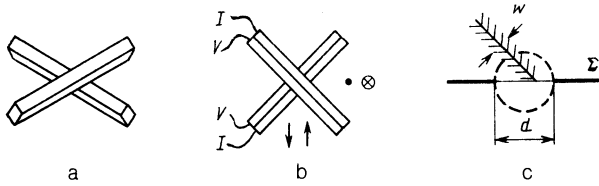


FIG. 1. Experimental geometry: a) configuration and mutual positions of electrodes used to form sliding contacts; b) electrodes in the contact plane (current and potential terminals are shown) and directions of relative displacement of electrodes used to form contacts (labeled by arrows and symbols); c) schematic representation of a contact in the form of a circular aperture with a thin screen Σ cut by a plane perpendicular to a twinning plane (d is the diameter of the aperture, w is the effective thickness of a twinning plane, and the dashed circle is the effective volume of the phonon generation region in the contact).

room temperature and in the course of mounting they were clamped so that one end was inside a miniature holder to which current and potential conductors were soldered. The electrode surfaces were electropolished before every cycle of measurements.

The measured characteristics were the contact resistance in the normal state R_0 at $V = 0$ and the voltages representing the first and second harmonics of the modulating signal $V_1(V)$ and $V_2(V)$. [The dependence $V_2(V) \propto d^2 V/dI^2(V)$ was called the point-contact spectrum.] The thermal and modulation broadening of the spectra was avoided by making all measurements at $T = 1.6$ K using a weak modulating signal described later by the initial value of the modulating voltage $V_{1,0}$. The superconductivity was destroyed by the application of a static magnetic field.

The experimental data were treated by transforming $V_2(V)$ to $\bar{V}_2(V) \propto d^2 I/dV^2(V)$ and eliminating the background (Fig. 2), which yielded the point-contact EPI function $g_{pc}(\omega)$ that differed from the Eliashberg EPI function $g(\omega)$ by the point-contact form factor in the integrand of an expression given in Ref. 5. The background was allowed for in the traditional manner⁶ and in accordance with the theory.⁷ (In the case of a high background level the numerical determination of the latter from the expression given in Ref. 7 became unstable.) Normalization of the absolute values of $g_{pc}(\omega)$ was carried out in the approximation of a quadratic and isotropic dispersion law of electrons, justified for this purpose in the case of nontransition metals,⁵ using a model of a contact in the form of a clean circular aperture ($d \ll l$, where d is the contact diameter and l is the mean free path of an electron). In such cases it follows in particular from the Sharvin expression that in the case of tin we have $d = 28R_0^{-1/2}$ nm if R_0 is measured in ohms. The measurement technique and the details of the procedure used to find the point-contact EPI function are given in Ref. 18.

In the course of recording and analysis of the spectra we determined the maximum of the voltage representing the second harmonic $V_{2,max}$, the background parameter $\bar{\gamma}$ equal to the ratio of \bar{V}_2 at the end of the EPI spectrum to its highest value within the spectrum, the maximum absolute value of the point-contact EPI function g_{pc}^{max} , the position of the absolute maximum $\hbar\omega(g_{pc}^{max})$, and the ratio of the intensities of the lf and hf maxima $g_{pc}(\omega)$ (at energies in the region of 6 and 15 meV) denoted arbitrarily as A/O, as well as the

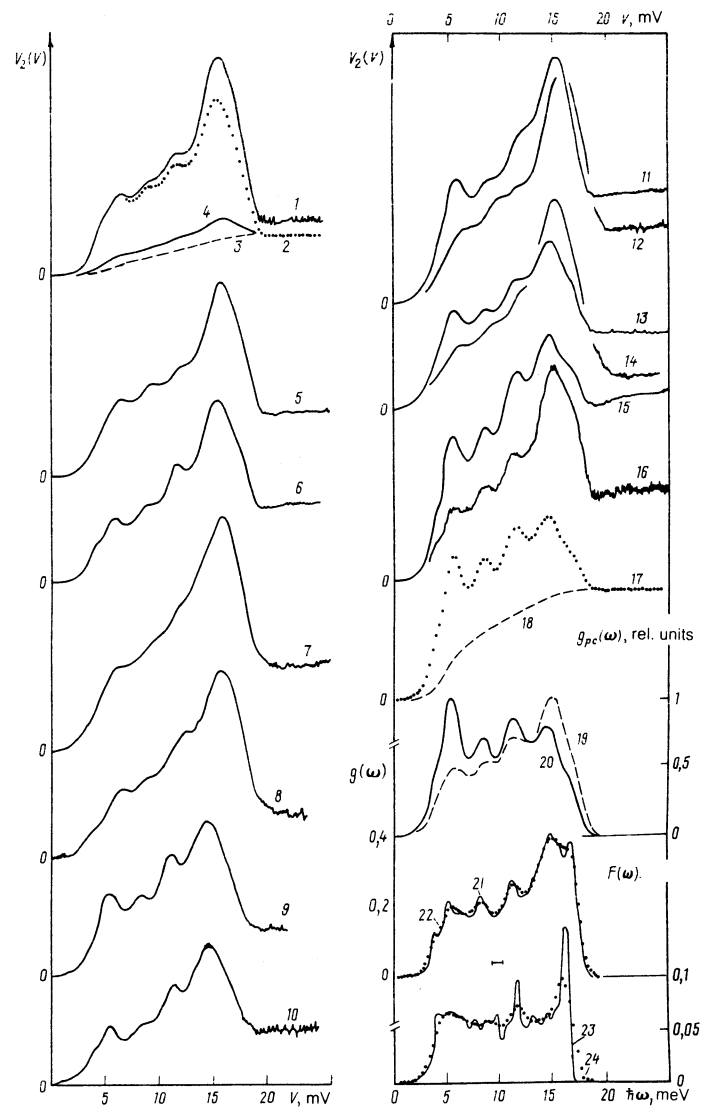


FIG. 2. Point-contact EPI spectra $V_2(V) \propto d^2 V/dI^2(V)$ obtained for contacts between undeformed single-crystal electrodes (curves 1 and 5–10) and electrodes with twinning planes (curves 11–16), main dependences determined in the course of reconstruction of the point-contact EPI function (curves 2–4 and 17–18), EPI functions (curves 19–22) and densities of phonon states (curves 23 and 24): 1, 5–6) spectra of contacts between unoriented electrodes (with random orientation of the contact axis and of principal crystallographic directions of bank electrodes); 7–8) contact axis oriented along [100] in both electrodes; 9–10) contact axis oriented along [001] in both electrodes; 11–12), 13–14), 15–16) pairs of spectra each of which represents two adjacent contacts (with distances between the contacts exceeding the separation between twinning planes); 2), 17) $\bar{V}_2(V) \propto d^2 I/dV^2(V)$ for curves 1 and 15; 3), 15) background⁶ for curves 1 and 15; 4) background⁷ for curve 1; 19), 20) point-contact EPI functions reconstructed from spectra 1 and 15, respectively; 21) Eliashberg EPI function obtained by the tunnel effect method in Ref. 12; 23) calculations reported in Ref. 13; 22), 24) curves 21 and 23 replotted allowing for the same broadening (horizontal section with cuts) as for curves 19 and 20.

point-contact EPI constant λ_{pc} and the average phonon frequency $\langle\omega\rangle$. It should be stressed that the average phonon frequency is independent of the normalization of the EPI function and can be determined quite accurately from point-contact spectroscopic data.

Control experiments on undeformed electrons were used to determine the characteristics of contacts both between unoriented electrodes with a random orientation of the geometric elements and principal crystallographic directions and of those in which the axis was oriented along principal crystallographic directions [100] and [001]. In the case of unoriented electrodes (both deformed and undeformed) the role of the EPI anisotropy effects was revealed and allowed for by making several series of measurements. In each series one or both electrodes were remounted after rotation by 90° about the longitudinal axis of the electrode.

EXPERIMENTAL RESULTS AND DISCUSSION

In each series of measurements on deformed electrodes the majority of the results formed a typical group which did not exhibit any significant changes in the value of $\langle \omega \rangle$ or in the relative intensities of the maxima $g_{pc}(\omega)$ from one contact to another. Typical point-contact EPI functions differed only in respect of the maximum absolute intensity, which—being calculated using the model of a clean aperture—was found to be maximal for the cleanest contacts.⁵ One typical point-contact spectrum obtained in a different series of measurements is reproduced in Fig. 2 (curves 12, 14, and 16). These curves were selected because they were determined for contacts closest to those for which the EPI spectra were found to be untypical (curves 11, 13, 15). [The total number of contacts formed by deformed electrodes (≈ 200 pieces) was such that we expected ≈ 4 contacts to have one of the electrode banks in the region of a twinning plane.] The characteristics of the spectra were collected and listed in Table I.

A comparison of typical values of $\langle \omega \rangle$ belonging to different series revealed large and fully detectable differences, amounting to a few percent. These differences were nevertheless only at the level of the observed scatter of the values of $\langle \omega \rangle$ for contacts between unoriented and undeformed electrodes and less than the differences between the contacts formed by single crystals oriented along the principal crys-

tallographic directions (Table I). Therefore, the differences between typical data obtained in different series of measurements could be easily explained by the EPI anisotropy. A common feature of the point-contact EPI spectra of tin illustrated in Fig. 2 was the presence of four maxima at 6, 9, 12, and 15 mV, as well as “shoulders” or kinks at 4 and 17 mV. In the case of the same spectra the selection of different background functions in the reconstruction of $g_{pc}(\omega)$ had practically no effect on the average phonon frequency or on the positions of the relative intensities of the maxima of the point-contact EPI function (Table I). The arithmetic average and the error in the average of the integral values of $\langle \omega \rangle$ and λ_{pc} , obtained using ten $g_{pc}(\omega)$ functions with a high absolute intensity reconstructed from the characteristics of contacts between unoriented electrodes, amounted to $\overline{\langle \omega \rangle} = 9.52 \pm 0.01$ meV and $\overline{\lambda_{pc}} = 0.79 \pm 0.01$ (0.63 if an allowance was made for the background in accordance with Ref. 7).

The most important difference between the recorded untypical point-contact spectra, reflecting in our opinion the influence of twinning planes, was a strong softening of the EPI spectrum of a contact (Fig. 2), which could be described qualitatively by the value of the average phonon frequency, which was much less than for all the other point-contact EPI spectra of tin. There was a considerable increase in the relative intensity of the lf part of the spectrum, but the shift of the positions of the maxima in the spectrum toward lower energies was slight. No new modes were found in the anomalous point-contact EPI spectra.

Another distinguishing feature of untypical point-contact spectra was a considerable increase of the background level (as demonstrated clearly by pairwise comparison of curves 11–12, 13–14, and 15–16 in Fig. 2), but the high absolute intensity was still retained (Table I).

It is known⁷ that the background component of point-contact spectra is due to reabsorption of nonequilibrium phonons by electrons in a contact. In the case of dirty con-

TABLE I. Characteristics of point-contact spectra shown in Fig. 2.

No. of curve in Fig. 2	R_{∞}, Ω	$V_{1,0}, \mu V$	$V_{2max}, \mu V$	$\tilde{\gamma}$	g_{pc}^{max}	$\hbar\omega(g_{pc}^{max}), meV$	$A/0$	λ_{pc}	$\langle \omega \rangle, meV$
1	8,5	425	0,72	0,23	0,41 0,31 *	15,0 15,0 *	0,48 0,49 *	0,74 0,56 *	9,60 9,57 *
5	14,8	474	1,75	0,30	0,39 0,30 *	15,7 15,7 *	0,48 0,48 *	0,66 0,51 *	9,95 9,92 *
6	2,25	373	1,07	0,34	0,21 0,29 *	15,0 15,0 *	0,55 0,55 *	0,54 0,40 *	9,47 9,43 *
7	8,1	522	1,39	0,32	0,38 0,30 *	15,5 15,5 *	0,50 0,51 *	0,76 0,61 *	9,65 9,56 *
8	17,8	789	1,04	0,23	0,24 0,20 *	14,8 14,8 *	0,40 0,43 *	0,42 0,36 *	10,05 9,84 *
9	5,8	549	0,96	0,28	0,22 0,18 *	14,6 14,6 *	0,70 0,74 *	0,46 0,41 *	8,79 8,51 *
10	7,5	430	0,98	0,34	0,42 0,32 *	14,3 14,3 *	0,57 0,60 *	0,82 0,63 *	9,08 9,04 *
11	12,8	501	0,91	0,40	0,33 0,23 *	14,9 14,9 *	0,72 0,73 *	0,69 0,50 *	8,54 8,49 *
12	9,5	426	0,82	0,29	0,41 0,32 *	15,5 15,4 *	0,39 0,40 *	0,67 0,52 *	10,19 10,15 *
13	17,4	475	0,68	0,42	0,32 0,24 *	14,5 14,5 *	0,83 0,84 *	0,79 0,60 *	8,35 8,31 *
14	48,0	809	1,24	0,14	0,48 0,41 *	14,9 14,9 *	0,32 0,32 *	0,76 0,70 *	10,15 9,97 *
15	6,3	336	0,84	0,61	0,30	5,6	1,25	0,69	8,18
16	8,4	277	0,39	0,35	0,40 0,29 *	15,1 15,1 *	0,40 0,41 *	0,69 0,45 *	9,81 9,77 *

*Values obtained with allowance for the background according to Ref. 7.

tacts such a reabsorption is enhanced because the escape of phonons from the contact region is hindered.⁹ Usually contamination shortens the mean free path of electrons, which reduces the intensity in the point-contact spectrum.⁵ Such EPI spectra of tin were found to be characterized not only by a low intensity (with the value of the constant λ_{pc} , calculated using the model of a clean aperture, several times less than $\lambda_{pc}^{\max, \max}$), but also by an excess current in the superconducting state which differed little from that predicted by the theory of Ref. 10 in the dirty limit.²⁾ A quantitative analysis failed to reveal any significant deviations of $\langle \omega \rangle$ from the average value for clean contacts or any anomalous ratio of the intensities of the maxima of $g_{pc}(\omega)$

The high intensity in the point-contact spectra in the presence of a strong background is the property expected of a contact with an inhomogeneous distribution of scatterers (defects) concentrated at the periphery of the region where the electric current is concentrated.⁹ If structure defects are extended (twinning planes, grain boundaries, dislocations), they differ in respect of the strength of the scattering of electrons and phonons. Extended defects scatter strongly long-wavelength phonons and return them to the center of the region where the electric current is concentrated, which facilitates reabsorption of phonons by conduction electrons.

In the case of point contacts of typical dimensions (amounting to hundreds of angstroms) the presence of extended defects can hardly have any significant role. The majority of phonons generated by electrons when the bias voltage applied to a contact is of the order of the Debye energy have a wavelength of the order of the lattice constant and are therefore scattered by defects in the same way as electrons. A strong background in a high-intensity point-contact spectrum may then be due to point defects (or impurities) concentrated at the contact periphery. Such defects scatter strongly hf phonons and return them to the center of the contact resulting in an almost complete reabsorption of these phonons by electrons. However, the scattering of conduction electrons by these defects does not affect the intensity of the point-contact spectrum because of the positions of these defects at the contact periphery where the current density is low and where the electrical potential reaches a value close to that well inside the electrode. However, even this explanation fails to account for the experimental results reported above, because we should then observe conventional point-contact EPI spectra representing an unperturbed pure metal.

It seems most likely that the high background level together with the high density in our point-contact spectra and the anomalously low values of $\langle \omega \rangle$ are due to reabsorption of phonons located within twinning planes (Fig. 1c) and represents one of the proofs of their existence. The group velocity of such phonons is low and the "center of gravity" of the density of states is shifted toward lower frequencies.³ In principle, the background component of the spectrum may include also a contribution from the scattering of conduction electrons by electrons localized near twinning planes. The existence of such localized states is discussed by Khlyustikov and Buzdin in their review.³

The point-contact EPI function represented by curve 19 in Fig. 2 (reconstructed from the spectrum represented by curve 1, typical of a contact between unoriented electrodes) should—according to Ref. 11—describe satisfacto-

rily the EPI in a polycrystalline metal and is in good agreement with the isotropic Eliashberg EPI function (curve 21 in Fig. 2). Therefore, in the case of tin the distorting influence of the point-contact form factor on the relative intensities of the maxima of the EPI function can be regarded as negligible. The energy dependence of the EPI matrix element is also unimportant in the case of tin and the density of the phonon states $F(\omega)$ in Fig. 2 [and other reliable graphs of $F(\omega)$ reported in Ref. 5] exhibits—like the EPI functions represented by curves 19 and 21 in Fig. 2—a high-intensity hf peak.

An anomalous ratio of the intensities of the maxima of $g_{pc}(\omega)$, represented by curve 20 in Fig. 2 (obtained from an untypical spectrum) when the lf maximum becomes the principal one, cannot be explained by deviation of the contact properties from the clean aperture model. Thus, the results of calculations of point-contact EPI functions in zinc¹⁴ carried out using a model of a contact in the form of a long channel revealed a clearer (compared with the circular aperture model) structure of the hf singularities of $g_{pc}(\omega)$ and a lower intensity of the lf peak.

A considerable reduction in the value of $\langle \omega \rangle$ and the relative intensities of the maxima of the EPI function, similar to those observed for $g_{pc}(\omega)$ (curve 20 in Fig. 2), were established earlier by the tunnel effect method for amorphous^{15,16} and granulated¹⁷ thin films. Nevertheless, random amorphization of a metal at a point contact could not account for untypical EPI spectra, because it would have resulted in a strong scattering of electrons in a contact and, consequently, in a reduction of the intensity in the spectrum. In the opposite case the effects due to the amorphous state of a metal in a contact would have been detected by control experiments on undeformed electrodes. Moreover, amorphization is shown (see, for example, Ref. 16) to broaden the bands in the EPI spectra, which was not observed in the case of the anomalous point-contact spectra recorded by us (curves 11, 13, and 15 in Fig. 2).

The discrepancy between the values of λ_{pc} obtained for different contacts and different background functions (Table I) were somewhat higher than the scatter of the tunnel data reported by different authors (Table II). However, the value of $\overline{\lambda_{pc}, T_c} = 0.76$ found from $\langle \omega \rangle$ given above using the McMillan equation ($\mu^* = 0.13$ for $T_c = 3.72$ K—see Ref. 15) was in good agreement with the known values of λ (Table II) and was more reliable.

The change in the critical superconducting transition temperature δT_c in a narrow layer of a metal near a twinning plane with an effective thickness $w \sim 10a$ (a is the interatomic spacing) was undoubtedly of interest. We assumed that the anomalous behavior of some of the EPI spectra of con-

TABLE II. Integral characteristics of the electron phonon interaction obtained by the tunnel effect method.

Ref.	$\langle \omega \rangle$, meV	λ
12	9,50	0,72
18	8,63	0,862
16	9,4	0,70

tacts between deformed tin electrodes was due to the fact that a twinning plane was within the contact region and we estimated δT_c to the nearest order of magnitude using the McMillan equation. We first determined the value of λ_{pc} , T_c for $T_c = 3.72$ K and $\mu^* = 0.13$ using the values of $\langle\omega\rangle$ for an untypical EPI spectrum. (The use of T_c for bulk tin transformed this operation into an estimate of the lower width to λ_{pc} , T_c .) Then, we should allow for the fact that in the $d \gtrsim w$ case a twinning plane could occupy between one-half and one-quarter of the effective volume of the phonon generation region $\Omega \sim d^3$ associated with the electrode bank containing a twinning plane (Fig. 1c). In the rest of the region Ω we assumed that the EPI constant was $\overline{\lambda_{pc}, T_c}$ (exactly as in the case of a contact without a twinning plane) and that the contributions of the various parts of Ω was additive, which allowed us to determine more accurately the EPI constant in a layer of thickness w . Finally, using once again the same values of $\langle\omega\rangle$ and μ^* as before, we found that $\delta T_c \sim T_c$. This value of δT_c was in good agreement with the results of measurements made on samples composed of a fine-grained deformed tin powder with a particle size less than the coherence length,³ when the proximity effect was suppressed. In the light of the data of Ref. 4, it would be of interest to investigate further the EPI in deformed tin using samples with different angles at the vertices of twinning wedges and also near dislocations.

The authors are grateful to Yu. V. Sharvin for valuable discussions of their results.

¹ Were usually referred to simply as contacts.

² See also the correction to Ref. 10: which is given in Zh. Eksp. Teor. Fiz. 79, 2016 (1980) [Sov. Phys. JETP 52, 1018 (1980)].

- ¹ I. A. Gindin, M. B. Lazareva, V. I. Sokolenko, and Ya. D. Starodubov, Abstracts of Papers presented at the Low-Temperature Physics Conference, Kharkov, 1980 (LT-21) [in Russian], Part 1, p. 292.
- ² M. S. Khaikin and I. N. Khlyustikov, Pis'ma Zh. Eksp. Teor. Fiz. 33, 167 (1981) [JETP Lett. 33, 158 (1981)].
- ³ I. N. Khlyustikov and A. I. Buzdin, Usp. Fiz. Nauk 155, 47 (1988) [Sov. Phys. Usp. 31, 409 (1988)].
- ⁴ I. N. Khlyustikov, Zh. Eksp. Teor. Fiz. 96, 2073 (1989) [Sov. Phys. JETP 69, 1171 (1989)].
- ⁵ I. K. Yanson and A. V. Khotkevich, *Atlas of Point-Contact Spectra of the Electron-Phonon Interaction in Metals* [in Russian], Naukova Dumka, Kiev (1986).
- ⁶ I. K. Yanson, I. O. Kulik, and A. G. Batrak, J. Low Temp. Phys. 42, 527 (1981).
- ⁷ I. O. Kulik, Fiz. Nizk. Temp. 11, 937 (1985) [Sov. J. Low Temp. Phys. 11, 516 (1985)].
- ⁸ S. N. Kraïnyukov, A. V. Khotkevich, I. K. Yanson *et al.*, Fiz. Nizk. Temp. 14, 235 (1988) [Sov. J. Low Temp. Phys. 14, 127 (1988)].
- ⁹ I. O. Kulik, A. N. Omel'yanchuk, and I. K. Yanson, Fiz. Nizk. Temp. 7, 263 (1981) [Sov. J. Low Temp. Phys. 7, 129 (1981)].
- ¹⁰ A. V. Zaitsev, Zh. Eksp. Teor. Fiz. 78, 221 (1980) [Sov. Phys. JETP 51, 111 (1980)].
- ¹¹ S. N. Kraïnyukov, A. V. Khotkevich, Yu. L. Shitikov *et al.*, Fiz. Met. Metalloved. 67, 1117 (1989).
- ¹² J. M. Rowell, W. L. McMillan, and W. L. Feldmann, Phys. Rev. B 3, 4065 (1971).
- ¹³ R. R. Rao and J. V. S. S. Narayanamurthy, Indian J. Pure Appl. Phys. 23, 16 (1985).
- ¹⁴ A. P. Zhernov and A. E. Trenin, Fiz. Tverd. Tela (Leningrad) 27, 3543 (1985) [Sov. Phys. Solid State 27, 2136 (1985)].
- ¹⁵ N. V. Zavaritskiĭ, Usp. Fiz. Nauk 108, 241 (1972) [Sov. Phys. Usp. 15, 608 (1973)].
- ¹⁶ K. Knorr and N. Barth, J. Low Temp. Phys. 4, 469 (1971).
- ¹⁷ V. M. Svistunov, O. V. Grigut', Yu. F. Revenko, and A. I. D'yachenko, Abstracts of Papers presented at Conf. on Low-Temperature Physics, Leningrad, 1988 (LT-35) [in Russian], Part 1, p. 151.
- ¹⁸ E. L. Moore, R. W. Reed, and F. G. Brickwedde, Phys. Rev. B 15, 187 (1977).

Translated by A. Tybulewicz